International Journal of Biological Macromolecules 235 (2023) 123849

Contents lists available at ScienceDirect

International Journal of Biological Macromolecules

journal homepage: www.elsevier.com/locate/ijbiomac

Evaluation of chitosan salt properties in the production of AgNPs materials with antibacterial activity

I. Aranaz [a,c,*], F. Navarro-García [b], M. Morri [d], N. Acosta [a,c], L. Casettari [d], A. Heras [a,c]

[a] Departamento de Química en Ciencias Farmacéuticas, Facultad de Farmacia, Universidad Complutense de Madrid, Plaza de Ramón y Cajal s/n, E-28040 Madrid, Spain
[b] Departamento de Microbiología y Parasitología, Facultad de Farmacia, Universidad Complutense de Madrid, Plaza de Ramón y Cajal s/n, E-28040 Madrid, Spain
[c] Instituto Pluridisciplinar, Universidad Complutense de Madrid, Paseo Juan XXIII, num. 1, E-28040 Madrid, Spain
[d] Department of Biomolecular Sciences, School of Pharmacy, University of Urbino Carlo Bo, Piazza del Rinascimento, 6, 61029 Urbino, PU, Italy

ARTICLE INFO

Keywords:
Chitosan
Silver nanoparticles
Nanocomposite

ABSTRACT

In this study, water-soluble chitosan salts (chitosan amine sulfopropyl salts) were prepared from chitosan samples with different molecular weights and deacetylation degrees. These soluble-in-water polymer salts allowed us to produce, in an eco-friendly and facile method, silver nanoparticles (AgNPs) with better control on size and polydispersity, even at large silver concentrations than their corresponding chitosan sample. Chitosan salt-based materials (films and scaffolds) were analyzed in terms of antibacterial properties against *Staphylococcus aureus* ATCC23915 or *Pseudomonas aeruginosa* ATCC 27853. 3D scaffolds enhanced the effect of the chitosan-AgNPs combination compared to the equivalent films.

1. Introduction

The antimicrobial activity of silver has been well-known since ancient times. The earliest evidence of the use of silver for therapeutic purposes dates back to the Han Dynasty in China; texts from Hippocrates described the use of silver in wound healing, and silver vessels were used to make water potable in the Phoenician empire [1–3]. Silver has been used in the form of metallic silver, silver nitrate or silver sulfadiazine in treating burns, wounds and different infections. In particular, treating wounds with silver was common from the 1800s to the mid-1900s. However, the use of silver and other non-antibiotic treatments diminished with the discovery of penicillin and other highly effective antibiotics against bacterial infection. Today, due to the emergence of antibiotic-resistant strains, interest in non-antibiotic treatments such as silver is gaining attention again [4]. Nanosized metallic particles are unique and can considerably change physical, chemical, and biological properties compared to bulk materials. Silver nanoparticles have proven to be efficient antimicrobial entities due to their large surface area-to-volume ratio [5]. Silver nanoparticle synthesis can be carried out by physical, chemical or physicochemical methods [6,7]. Physical approaches include the use of heat, plasma or ultrasound radiation, among others [8–10]. This approach exhibits high speed and low chemical consumption, but these processes are highly energy-demanding, require specialized types of equipment, the yields are low and the samples are highly polydisperse.

The chemical approach needs a metal precursor, a reducing agent and a stabilizing/capping agent [11]. Most chemical AgNPs production processes are based on citrate (Turkevich method), borohydride reduction, Tollens reaction and polyol reaction [6]. Citrate reduction is fast and cost-effective, but borohydride reduction allows better size and shape control. Although these methods are more accessible than physical ones and exhibit large yields, they use hazardous chemicals and the production of high-purity nanoparticles is difficult since the chemicals tend to fix the surface of the nanoparticles. Therefore, the synthesis of AgNPs by chemical reduction of Ag+ is a non-expensive process that requires using green strategies for biomedical applications to avoid using hazardous chemicals and solvents. It is possible to find numerous reports on silver nanoparticle synthesis using stabilizers of natural origin, such as soybean polysaccharides, chitin, chitosan, heparin and starch, among others [12–16].

Among them, chitosan is a biodegradable and biocompatible polymer obtained by the deacetylation of chitin, one of the most common polymers in nature. Due to its natural origin, chitosan cannot be defined as a ubiquitous molecule but as a family of copolymers of *N*-

Abbreviation: AgNPs, silver nanoparticles.

* Corresponding author at: Departamento de Química en Ciencias Farmacéuticas, Facultad de Farmacia, Universidad Complutense de Madrid, Plaza de Ramón y Cajal s/n, E-28040 Madrid, Spain.
E-mail address: iaranaz@ucm.es (I. Aranaz).

https://doi.org/10.1016/j.ijbiomac.2023.123849
Received 6 October 2022; Received in revised form 12 February 2023; Accepted 23 February 2023
Available online 27 February 2023

acetylglucosamine and glucosamine. Chitosan has been used in several fields, such as biocatalysts, the food industry, biomedicine, pharmacy, and agriculture [17].

Chitosan is soluble in aqueous acid solution and can be readily manufactured in different technological forms such as films, micro and nanoparticles, sponges, threads, or hydrogels for a large variety of applications [18–22]. In the pharmaceutical field, properties such as biocompatibility, biodegradability and wound healing make this polymer a molecule of great interest [23]. Chitosan was added to the list of excipients in the USP in 2011, and it also appears in the EU Pharmacopeia, boosting the interest in this polymer in pharmaceutical and biomedical applications [24,25]. However, chitosan has some limitations like its lack of solubility in physiological pH, and therefore, modifications in the molecule need to be carried out. These chitosan derivatives are also very promising molecules in the field of biomedical applications since they are designed to improve chitosan properties such as water solubility, mucoadhesion or antimicrobial activity, among others [26–28].

Several reports can be found in the literature exploring the use of chitosan as AgNPs stabilizer [29,30] or as a reducing and stabilizer agent [31,32]. The production of AgNPs using chitosan both as a reducing agent and stabilizer is a complex issue due to the lack of homogeneity in the results. Chitosan-reducing properties seem to be related to the polymer physicochemical properties (molecular weight and deacetylation degree) and the method of the polymer obtention [33,34]. Other parameters, such as polymer or silver concentration, also affect the final result since chitosan rendered highly viscous gels or even precipitate in the presence of $AgNO_3$ solutions due to its chelating properties at room temperature. Some studies have shown that pH plays a fundamental role in forming AgNPs controlling size, polydispersity and stability [35,36]. Studies showed that acid media produced larger and polydisperse nanoparticles, and some authors have produced the silver AgNPs using chitosan suspensions in basic media [37,38]. Another approach is the use of soluble chitosan derivatives that avoid the use of acid pH. Chitosan hydrochloride salt solutions were not compatible with $AgNO_3$ since AgCl precipitated. Twu and coworkers have tested several chitosan salts and water-soluble derivatives to produce silver nanoparticles [37]. Depending on chitosan molecular chitosan, chitosan acetic salt and chitosan nitric salt solutions rendered highly viscous gels in the presence of $AgNO_3$ solutions at room temperature. *N*-carboxymethyl chitosan was water soluble and formed a large insoluble silver chelate after adding $AgNO_3$ solution. Other derivatives have been used to stabilize the silver nanoparticles once produced by chemical reduction. For instance, trimethyl chitosan nitrate has successfully stabilized silver nanoparticles using glucose as a reducing agent [27]. Although these derivatives successfully stabilized the nanoparticles, the use of extra chemicals is a disadvantage from the point of view of simplicity and sample purity. Furthermore, some processes used for the preparation of chitosan derivatives cost a great deal of time since multi-step processes are needed in their synthesis (i.e. trimethyl chitosan nitrate, enzymatically produced low molecular weight chitosan) or the use of energy-consuming equipment such as ultrasonic bath is needed (i.e. chitosan-poly(3-hydroxybutyrate); gallic acid-conjugated chitosan) [27,39,40].

Among chitosan derivatives, chitosan salt produced by the reaction of chitosan and propane sultone is gaining interest in biomedical applications due to the simplicity of its chemistry, its good water solubility, its antibacterial and antifungal activities [41], and its antibiofilm properties [42]. Although this chitosan derivative is identified as N-(3-sulfopropyl)chitosan salt, recently, a detailed study of the reaction has determined that the final product depends on the pH of the reaction [43]. When the reaction is carried out at acidic pH, the product is a mixture of N-(3-sulfopropyl)chitosan salt (covalent derivative) and sulfopropyl chitosan salt (ionic derivative) while N-(3-sulfopropyl)chitosan salt is mainly produced at basic media. The ionic derivative is soluble in water and does not precipitate or form gels in the presence of silver ions, so it is a potential candidate to be tested as a reducing agent and stabilizer in synthesizing silver nanoparticles. Therefore, this paper aims to evaluate, for the first time, the ability of chitosan ionic sulfopropyl salt to produce and stabilize silver nanoparticles by controlling both size and nanoparticle distribution and to determine their antimicrobial activity both in solution and as part of polymeric materials (scaffolds and films). We hypothesize that chitosan salt may contribute to the production of stable silver nanoparticles (AgNPs) with controlled size and polydispersity, particularly when water is used as a solvent. Moreover, manufacturing AgNP-chitosan in the form of 3D scaffolds may increase the antibacterial activity compared to AgNP-chitosan films due to a large surface.

2. Materials and methods

2.1. Materials

Chitosan (CHT1) was kindly donated by InFiQuS S.L. (Madrid, Spain). Polymer characterization data is shown in Table 1. Propane sultone, KNO_2 and $AgNO_3$ (purity $\geq$ 99.0 %) were purchased from Sigma-Aldrich (St. Louis, MO, USA). Methanol, acetic acid and HCl were purchased from Panreac (Madrid, Spain).

2.2. Chitosan depolymerization

Chitosan was chemically depolymerized with KNO_2/HCl to produce the sample denoted as CHT2 [44]. Briefly, the polymer was dissolved in HCl 0.1 M at 1 % *w/v* overnight, and a freshly prepared KNO_2 solution in water (31.36 mM) was added in a volume ratio of 1:27. The polymer depolymerization was carried out at 37 °C for 30 min. To stop the reaction and recover the depolymerized chitosan, a solution of NaOH in water (10 M) was dropped under stirring until a pH of 8–9 was reached. Finally, the solid polymer was recovered by filtration, it was thoroughly washed with milli-Q water and dried at 45 °C.

2.3. Chitosan reacetylation

As previously described, Chitosan was reacetylated with anhydride acetic to produce the sample CHT3 [45]. In brief, chitosan (2 % *w/v*) was dissolved in acetic acid 0.1 M and MeOH (ratio 1:1) was slowly added to this solution. A stoichiometric amount of anhydride acetic dissolved in MeOH (1 mL) was added to the chitosan-MeOH solution and the reaction was carried out for 24 h at room temperature. The polymer was precipitated by adding ammonia dropwise until pH 8 was reached. The precipitate was thoroughly washed with milli-Q water and dried at 45 °C.

2.4. Chitosan modification with propane sultone

Chitosan samples (CHT1, CHT2 and CHT3) were dissolved in acetic acid 0.2 M and heated at 60 °C, propane sultone was added to this media (chitosan amino group: propane sultone molar ratio 1:1), and the mixture was stirred for 6 h at 60 °C. After that, the mixture was transferred into a dialysis membrane (MWCO 3.5 kDa), and the samples were dialyzed against milli-Q water for 5 days changing the media every 12 h [43]. Chitosan derivatives (CHT1-S, CHT2-S and CHT3-S) were recovered by lyophilization (Telstar LyoQuest 55). In all cases, the recovered polymers were soluble in water, which indicates chitosan salt formation.

2.5. Polymer characterization

The chitosan acetylation degree was determined by the UV-first derivative spectroscopy method [46]. Chitosan viscosity average molecular weight (Mv) was determined by viscosity measurements and using the Mark-Houwink relationship. Chitosan samples were dissolved in 0.3 M AcOH/0.2 M AcONa [47], while chitosan sulphated samples were dissolved in NaCl 0.1 M [48,49].

Table 1
Main properties of chitosan and chitosan derivatives.

Sample	DA	η (dL/g)	Mv (kDa)	CrI (%)	S (%)	T max[1] (°C)	H (%)	T max [2] (°C)
CHT1	9.0	2.88 ± 0.17	58	61	–	65.19	10.74 (188.85 °C)	297.00
CHT2	7.0	1.16 ± 0.09	18	69	–	62.82	11.11 (179.57 °C)	299.68
CHT3	23.0	1.83 ± 0.05	31	62	–	61.63	10.06 (190.45 °C)	292.97
CHT1-S	–	0.94 ± 0.03	67	24	6.36	51.17	9.06 (105.88 °C)	241.01
CHT2-S	–	0.81 ± 0.02	58	27	7.06	57.25	9.20 (114.36 °C)	237.57
CHT3-S	–	0.30 ± 0.01	21	22	6.18	60.45	9.59 (115.76°°C)	237.27

DA: Acetylation degree, MV: viscous molecular weight, CrI crystallinity index; S: sulphur content; T max: T determined as maximum in DGT curves. Humidity was determined as the weight lost at the end of the first weight loss. End-point temperature for humidity is shown in brackets.

X-ray diffraction patterns were obtained using an x-ray diffractometer (PHILIPS X'PERT SW) with a copper anode at room temperature. The samples were scanned continuously from 5° to 50° 2θ angle at 45 kV and 40 mA. The crystallinity index (CrI) was determined according to Eq. (1) [50]

$$CrI = \frac{I110 - Iam}{I110} * 100 \quad (1)$$

where I_{110} = crystallinity diffraction pattern intensity at 2θ = 20° and I_{am} = amorphous diffraction pattern intensity at 2θ = 16°.

The sulphur content was determined by elemental analysis (LECO, CHNS-932) at CAI of Elemental Microanalysis at Complutense University.

ATR-FTIR measurements were carried out using a Cary 630 FTIR Spectrometer. Samples were analyzed at room temperature in the range between 450 and 4000 cm^{-1} with 20 scans.

Thermal analysis of the chitosan samples and the derivatives was carried out in a nitrogen atmosphere. Thermogravimetric (TG) and differential (DTG) thermogravimetric studies were carried out with a TA Instruments SDT Q600 system. All analyses were performed with around 4 mg sample in aluminium pans under dynamic nitrogen (20 mL) between 25 and 900 °C. The experiments were run at a scanning rate of 10 K/min.

For ^{1}H NMR and ^{13}C NMR analysis, around 10 or 20 mg of the polymers were diluted in 1 mL of D_2O or D_2O/DCl, and the spectra were recorded at room temperature in a Bruker AV 500 MHz system.

2.6. Silver nanoparticle synthesis and characterization

$AgNO_3$ dissolved in water (1 mM, 5 mM, 10 mM, 25 mM and 50 mM) was mixed with the polymer solution (1 %) dissolved in 0.1 M acetic acid (chitosan) or Milli Q water (chitosan salt). This rendered silver concentrations in the polymeric solutions of 0.166, 0.83, 1.66, 4.15 and 8.3 mM, respectively. The mixtures were heated at 90 °C for 5 h and the formation of AgNPs within the chitosan and chitosan salt solutions was followed by the appearance of the characteristic Ag exciton peak around 400 nm [33] in a UV–Vis spectrometer (Specord 205, Analityk Jena AG, Jena, Germany). AgNPs zeta potential was determined by Laser Doppler Electrophoresis in triplicates in a Nano-Zetasizer system (Malvern Panalytical's, Malvern, UK).

AgNPs morphology and size were evaluated under Transmission Electronic Microscopy (JEOL JSM 6335F, Tokyo, Japan) while the crystalline structure was elucidated by Selected Area Electron Diffraction (SAED) at ICTS National Centre of Electronic Microscopy (Complutense University). TEM images were analyzed with ImageJ software (National Institutes of Health, USA), and histograms were generated with Origin Pro 2021 software (OriginLab Corporation, Northampton, MA, USA). At least 50 representative nanoparticles per sample were analyzed to produce the histograms.

2.7. Film preparation

Polymeric solutions containing silver nanoparticles (silver concentration in the polymeric solution was 0.83, 4.15 and 8.3 mM) were mixed with a genipin solution in water (5 $mg{\cdot}mL^{-1}$), and the mixture was stirred for 10 min. 100 μL of each solution was placed into a 96 multiwell plate, and the films were produced by solvent casting methodology by allowing the samples to dry at room temperature for 48 h. Films were kept at room temperature in dark conditions until further assays.

2.8. Scaffold preparation

Polymeric solutions containing silver nanoparticles (0.83 or 8.3 mM silver concentration) were mixed with a genipin solution in water (5 $mg{\cdot}mL^{-1}$), and the mixture was stirred for 10 min. The solutions were frozen at −80 °C and lyophilized at −50 °C (Telstar LyoQuest 55, Azbil Telstar, Japan). Scaffolds were kept at room temperature in dark conditions until further assays.

2.9. Silver release

The release of the AgNPs from films and scaffolds in phosphate buffer saline (PBS) and phosphate buffer at pH 7.4 was evaluated. A known amount of the film or the scaffold was put in 2 mL of buffer at 37 °C under orbital stirring (100 rpm). Buffer was completely removed at different times (1, 2, 3, 4, 6 and 24 h) and fresh buffer was added. The removed buffer solution was diluted in HNO_3 0.1 M and filtered through a 0.45 mm regenerated cellulose filter (Albet, Relliehausen, Germany) before silver content determination by inductively coupled plasma mass spectrometry using an OPTIMA 2100 DV spectrometer (PERKIN ELMER, Waltham, MA, USA). Each experiment was carried out in triplicates.

2.10. Antimicrobial activity

Minimal inhibitory concentration (MIC) was evaluated in microwell plates according to CLSI standards [51]. Briefly, the activity of two-fold dilution amounts of the compounds was tested against $\sim 5{\cdot}10^4$ cells per well of either *Staphylococcus aureus* ATCC23915 or *Pseudomonas aeruginosa* ATCC 27853 at 37 °C for ≥18 h in Mueller-Hinton broth (MHB, Laboratorios Conda, Spain). Those wells with the lowest amount of the products showing no visible growth (measured at 595 nm in a Biorad Model 680 microplate reader) were recorded as the MIC. The content of the wells showing no growth was tenfold diluted in MHB (final volume 2 mL), to dilute 10 times the AgNPs concentration and allow the recovery of those cells whose growth was stopped but not killed, and incubated at 37 °C and 150 rpm for 18–24 h. After that, tubes with no visible growth were considered to harbour minimal bactericidal concentration (MBC).

The activity of scaffolds or films was evaluated in triplicate by including one piece of each type in tubes containing 2 mL MHB inoculated with $6.25{\cdot}10^5$ $cells{\cdot}mL^{-1}$ of either *S. aureus* or *P. aeruginosa*. Growth was visually inspected after incubation at 37 °C for 24, 48 and 120 h in an orbital shaker at 170 rpm. After 24 h, bacterial inhibition in tubes showing no apparent growth was evaluated by plating tenfold serial dilutions onto MH plates and incubating at 37 °C for an additional period of 24 h.

To detect the activity of AgNPs upon release from scaffolds, scaffolds

were immersed in sterile MHB and incubated at 37 °C and 170 rpm using Ag^+ solutions at the same concentration as controls. Samples at different times (0, 0.5, 1, 1.5, 2, 3, 4, 6, 9 and 24 h) were isolated and assayed in a microwell assay. 96-well plates were inoculated with ~$5{\cdot}10^4$ bacteria per well, either with *P. aeruginosa* or *S. aureus* and incubated for 24 h at 37 °C and 200 rpm in a SPECTROstar Nano (BMG LABTECH GmbH, Biogen Cientifica SL, Spain) recording bacterial growth every 30 min. Growth curves were analyzed using MARS v3.3 (BMG LABTECH GmbH).

In addition, after 24 h of release (24 h), scaffolds were rescued from tubes, washed with MHB and immersed in fresh MHB to detect the remaining activity. Released samples were obtained from these tubes after 24 and 48 additional hours (Samples denoted as "24 N h" and "48 N h"). 24 h, 24 N h and 48 N h samples were assayed as above in triplicate, calculating the percentage of inhibition after 10 h of growth compared to the non-treated control. A two-way ANOVA was performed to detect statistically significant differences at $p < 0.05$ using GraphPad Prism 6.0.

3. Results and discussion

3.1. Chitosan salt production

In this work, a chitosan sample (CHT1) was depolymerized (CHT2) and reacetylated (CHT3) to obtain three chitosan samples with different physicochemical properties, as shown in Table 1. These samples were used as starting material to prepare three sulfonated-chitosan salts whose properties are also summarized in Table 1. In Fig. 1A inset, the typical ^{1}H NMR spectrum from chitosan in D_2O/DCl was observed, the signal at 2.4 ppm was ascribed to acetyl groups, and the signals at 4.0–4.3 ppm were assigned to the H-2, H-3, H-4, H-5, and H-6 of chitosan GluNAC moieties and signal at 3.2 was assigned to H-2 of chitosan GluN moiety. In the chitosan derivatives dissolved in D_2O, the signals occurring at 2.2–2.3, 3.2–3.3 and 4.0–4.1 ppm arose from three kinds of —CH_2 on the sulfopropyl group (Denoted with * in Fig. 1A). Sulphur contents determined by elementary analysis ranged from 6 to 7 % also confirming the presence of sulfopropyl moiety.

It has been widely reported that chitosan can be modified with propane sultone to render a soluble derivative identified as N-sulfopropyl chitosan [52,53]. However, Heydari et al. [43] have recently evaluated this reaction in detail, finding that the main product at acid pH was not the covalent derivative but a salt; since the hydrolysis of propane sultone, which occurs in acid media, produces negatively charged sulfopropyl groups that bound to N-sulfopropyl-chitosan chains producing a mixture of covalently modified chain (around 5 %) and sulfopropyl salt (around 95 %). To determine in more detail the composition of the samples produced in this work (sulfopropyl salt, covalent derivative or mixture of both), exhaustive dialysis (7 days changing media every day) of the derivatives against a basic media (pH around 10) was carried out. We analyzed the samples by ^{1}H NMR and ^{13}C NMR to elucidate their composition. In Fig. 1 (B, D), it is clearly observed the presence of the sulfopropyl chain in our sample (denoted with * in the figure) before the dialysis in basic media, while these

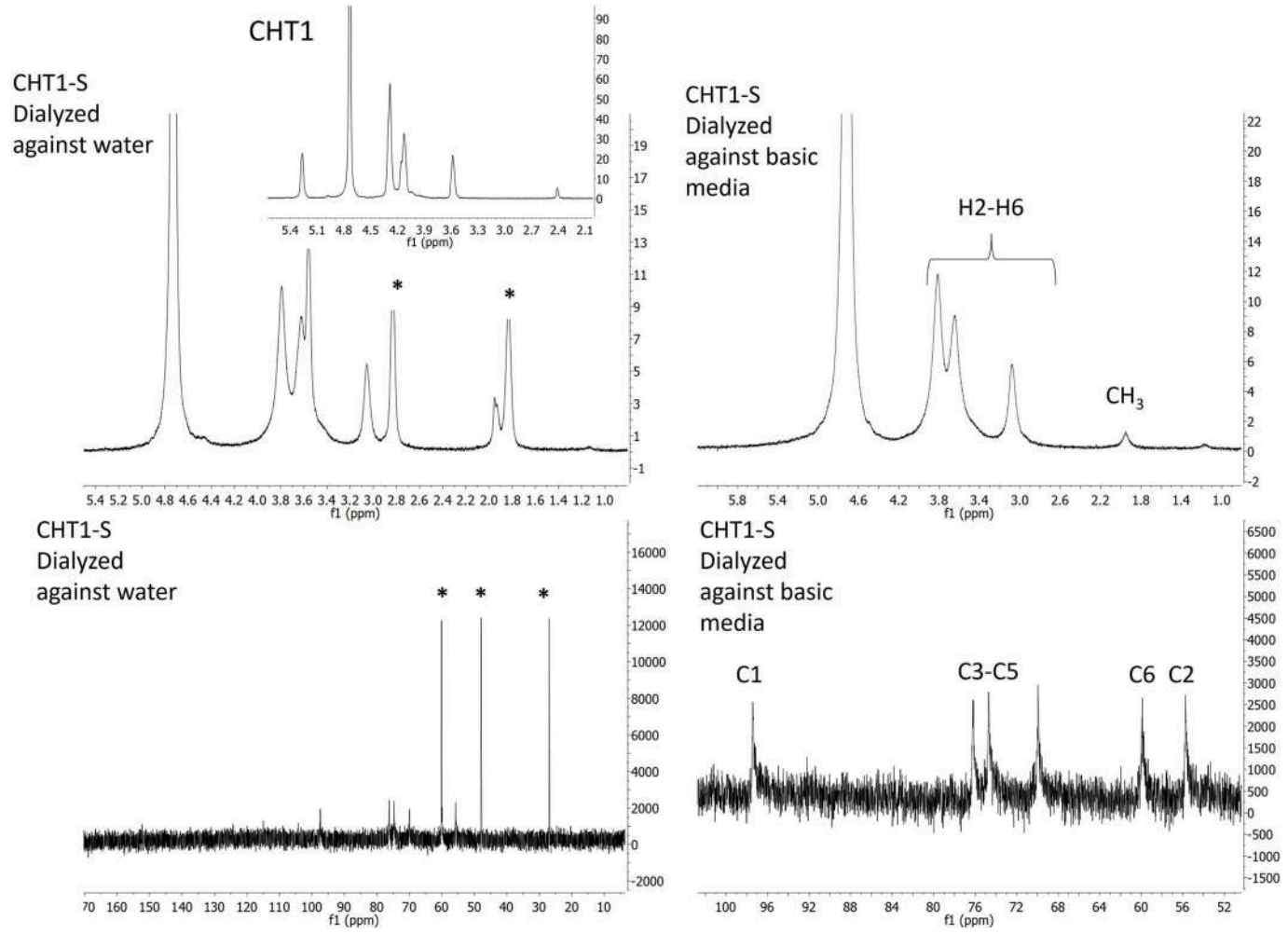

Fig. 1. Liquid ^{1}H NMR in D_2O/DCl of samples CHT1-S dialyzed against water (A) and basic media (B). Liquid ^{13}C NMR in D_2O/DCl of samples CHT1-S dialyzed against water (C) and basic media (C). Inset in panel A) Liquid ^{1}H NMR in D_2O/DCl of sample CHT1.

signals disappeared in the sample once it was dialyzed against basic media (Fig. 1 B, D). This indicates that the sulfopropyl group is ionically bonded to chitosan rather than covalently since under appropriate conditions was eliminated by dialysis.

These salts were further characterized in terms of composition by ATR-FTIR (Fig. 2).

The ATR-FTIR spectrum of sample CHT-2 is shown in Fig. 2 as an example of a chitosan spectrum. The broadband with a maximum at 3360 cm^{-1} and the shoulder at 3290 cm^{-1} confirmed the presence of —OH and —NH groups, respectively. The signal at 2871 cm-1 corresponded to —CH_2 stretching, at 1652 cm^{-1} —C═O stretching from amide I, at 1595 N-H bending from primary amide and —CO asymmetric stretching, the signal at 1425 cm^{-1} was assigned to —CH_2 bending, signals at 1053 cm^{-1} and 1156 cm^{-1} were assigned to C—O stretching, the signal at 1026 cm^{-1} was assigned to —C—O—C— stretching and signals at 886 were assigned to C—H bonds. All these bands correspond with chitosan ones [54].

In the derivatives, new bands appeared, while others were slightly modified in their position. Modification in the chitosan primary amino group was shown since the signal at 3360 cm^{-1} maintained its position while the signal at 3290 cm^{-1} disappeared. The band at 2871 cm^{-1} of chitosan was assigned to —CH_2 stretching split, and two new bands at 2907 cm^{-1} and 2881 cm^{-1} emerged. Bands around 532–662 cm^{-1} appeared due to the presence of sulphate groups [55,56].

Chitosan salts exhibited lower crystallinity than their corresponding parent chitosan due to the interaction of the negative charge of the hydroxyl propane sulfonate chain with the positive charge of the primary amine group on the chitosan backbone. The chitosan salts were also less viscous and were soluble in water at least up to 2 % *w/v*, while parent chitosan samples were not. Thermal analysis of chitosan and chitosan derivatives was also carried out (Table 1). For chitosan samples, weight loss occurred in two stages. The first one showed a maximum in DTG curves around 61–65 °C. This stage has been related to the strong affinity of polysaccharides for water molecules. The second one was observed around 300 °C and has been related to chitosan decomposition. These data are in good agreement with previously reported data [57]. In the case of chitosan salts, the first stage appeared around 50–60 °C and the second one around 240 °C. Polysaccharides usually show a strong affinity for water, and this behaviour was also observed in the chitosan salts with similar percentages of humidity; however, while this water was strongly bonded to chitosan and high temperatures were needed to remove it, in the case of the salts, the water was removed from the polymer at lower temperatures.

3.2. Colloidal AgNPs formation and characterization

The ability of chitosan to produce metallic nanoparticles acting both as reducing and stabilizing agent is well described in the literature. However, the control of the AgNPs characteristics, such as nanoparticle size or polydispersity, depends on the physicochemical properties of the polymer or even on the method used to produce it, as recently reported [33]. Therefore, firstly, we evaluated the ability of the three chitosan samples (parent, depolymerized or reacetylated) to produce the silver nanoparticles under thermal conditions. The colour of the polymeric solutions changed from transparent to brownish at low $AgNO_3$ concentrations (0.166–1.66 mM) and to dark grey at higher concentrations (4.15–8.3 mM), as shown in Fig. S1. The appearance of the AgNPs in the polymeric solutions was evaluated by following the typical surface plasmon resonance band (SPR) of the silver nanoparticles that appear around 400 nm. Symmetrical and narrow SPR band has been associated with AgNPs with a narrow interval of size and uniform shape [31]. As shown in Fig. 3 A, when using $AgNO_3$ 0.83 mM, a wide absorbance spectrum was observed in the chitosan sample, which indicates the presence of large AgNPs and polydispersity. Moreover, no exciton was observed at higher $AgNO_3$ concentration (4.15 mM) (Fig. S2). To improve the control in terms of AgNPs size and polydispersity, three water-soluble chitosan salts with different physicochemical properties (Table 1) were evaluated initially at 0.83 mM. Silver nanoparticle SPR bands in the chitosan salts solutions in water were clearly observed in contrast to chitosan solutions (Fig. 3 B), where broader spectra were observed. We did not find relevant differences in the FTIR-ATR spectra of AgNps-chitosan and AgNPs-chitosan salt samples that could explain why the latter can better control the size and polydispersity of the nanoparticles (Fig. S3). Chitosan derivatives exhibited a different ability to control silver nanoparticle production. AgNPs produced with sample CHT3-S exhibited a broad UV–vis spectrum with a maximum absorbance around 464 nm which indicated that the highly acetylated chitosan derivative had a poor control in the nanoparticle polydispersity and large aggregates were expected. On the contrary, AgNPs produced with samples with lower acetylation degree (CHT1-S and CHT2-S) showed narrower spectra with a maximum absorbance at 419 and 452 nm, respectively.

TEM micrographs revealed the presence of spherical nanoparticles along with some polyhedral nanoparticles whose size and polydispersity depended on the polymer characteristics (Fig. 3 C-E).

The histograms clearly showed that highly polydispersed nanoparticles were produced when using the highly acetylated derivative in

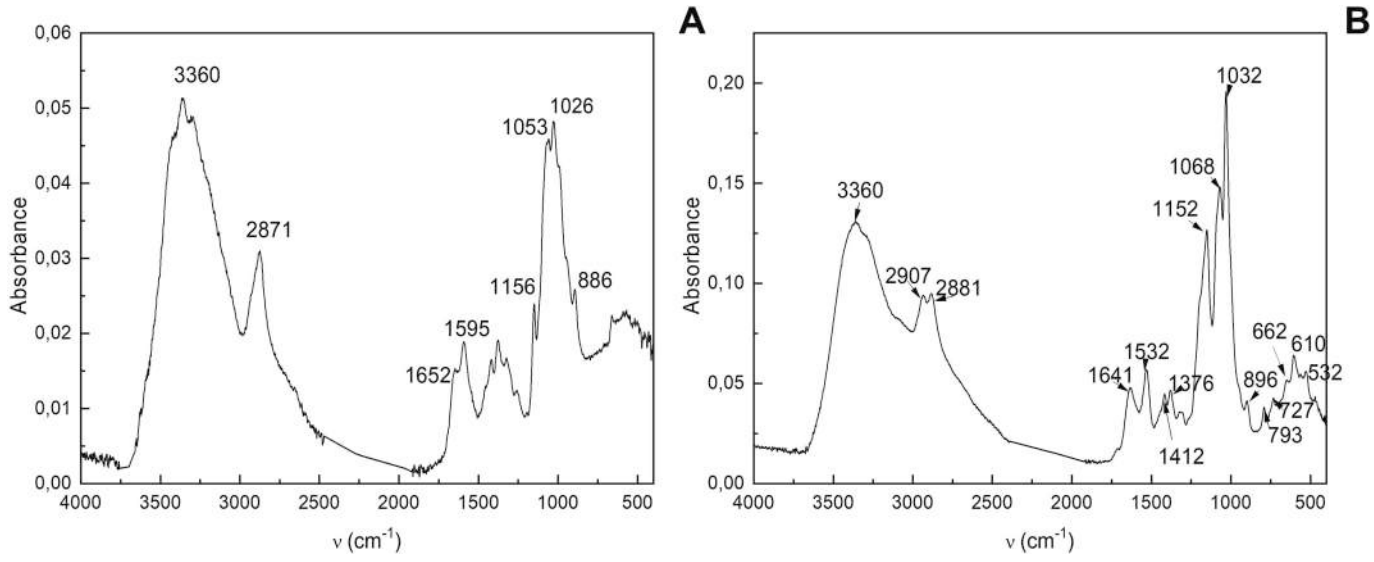

Fig. 2. ATR-FTIR Spectra of chitosan (A) and chitosan salt (B).

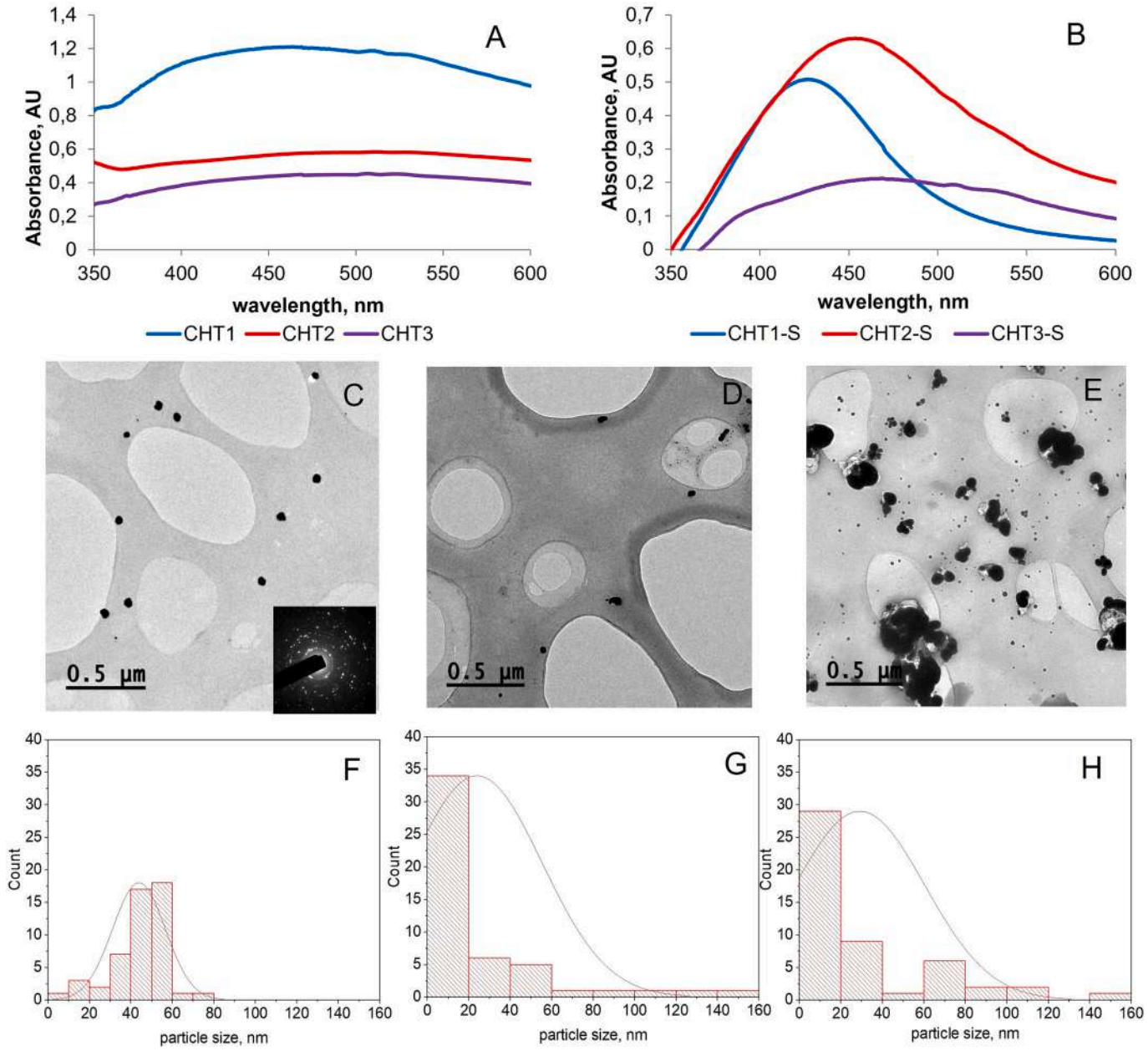

Fig. 3. UV–vis spectrum of silver-containing solutions (silver concentration 0.83 mM with chitosan dissolved in acetic acid (A) and chitosan derivatives dissolved in water (B)). TEM images of AgNPs (0.83 mM) produced with chitosan salts CHT1-S (C), CHT2-S (D) and CHT3-S (E). Inset Fig. 3 C: AgNPs SAED pattern. Size histograms of AgNPs colloidal solutions of CHT1-S (F), CHT2-S (G) and CHT3-S (H).

good agreement with the wide SPR band (Fig. 3 F, H). Comparing the samples with similar acetylation degrees, the higher molecular weight chitosan rendered nanoparticles with a larger size and better control in terms of polydispersity than the sample with lower molecular weight.

The crystalline nature of the AgNPs was determined from the selected area electron diffraction (SAED) patterns. An example of the SAED pattern is shown in Fig. 3 C (inset). AgNPs exhibited concentric rings in all samples, indicating that these nanoparticles were crystalline. By determining the spacing between rings, the planes 111, 200 and 311, which corresponded to FCC crystalline structure, were identified [58]. The zeta potential of the nanoparticles was approximately +40–45 mV in all samples, which is a good indicator of their colloidal stability.

Sample CHT1-S was selected to further optimize AgNPs production with silver concentrations in the polymeric solutions ranging from 0.166 mM to 8.3 mM (Fig. 4 left panel). The first point to be noticed was the ability of the chitosan salt solubilized in water to stabilize the AgNPs, even at large silver concentrations, as revealed by the presence of the silver SPR around 415–430 nm with an increment of the absorbance in the red region as the silver concentration increased. Parent chitosan could not produce silver nanoparticles with high silver concentration. In this sample, the solution turned dark grey and no SPR was observed (Figs. S1, and S2). We tested the formation of AgNPs using the water-soluble salt dissolved in acetic acid and we observed the presence of silver SPR but the maximum in the UV–vis spectra slightly shifted to red compared to the samples in water. This shift was indicative of the presence of large AgNPs and/or nanoparticle aggregation, indicating that water is a more appropriate solvent to control AgNPs size and stability (Fig. S2). The silver concentration did not remarkably affect the AgNPs' shape (Fig. 4). However, at 8.3 mM a large amount of AgNPs with particle sizes lower than 5 nm were observed, while this effect was not observed in the samples with lower concentrations. The AgNPs zeta potential ranged from +40 to +50 mV in all cases, with no relevant

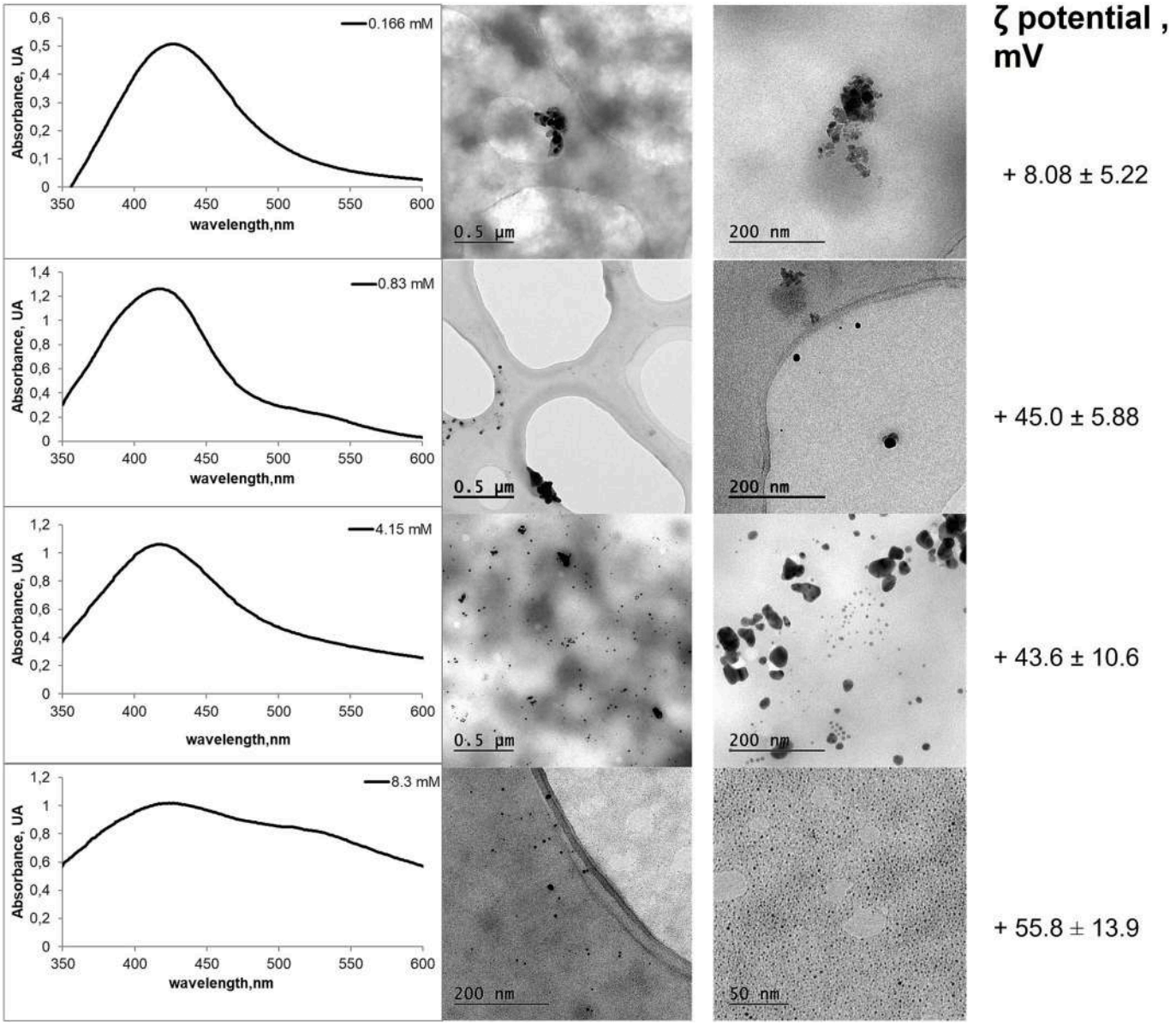

Fig. 4. Optical properties of AgNPs produced with different $AgNO_3$ concentrations using sample CHT1-S (0.166, 0.83, 4.15 and 8.3 mM). TEM of colloidal AgNPs produced with CHTS-1 sample at the different silver concentrations and zeta potential of the colloidal AgNPs.

differences among AgNPs produced using the three chitosan salt samples or silver concentration in the range 0.83–8.3 mM (Fig. 4 right panel). However, at a low silver concentration (0.166 mM), a lower positive zeta potential of around +8 mV was observed; therefore, they tended to aggregate as observed in TEM images.

3.3. Chitosan-based nanocomposites

Chitosan salts retained the filming properties of the parent chitosans, and films loaded with silver nanoparticles were easily produced by solvent-casting methodology. Films in PBS swelled to a large extent and were difficult to handle, so to improve their performance, films were crosslinked with genipin to avoid large swelling. In Fig. 5, the swelling of the crosslinked films is shown. Films produced with chitosan samples CHT2-S and CHT3-S samples showed higher swelling values than those produced with sample CHT1-S sample. The presence of AgNPs in the crosslinked films with genipin reduced the swelling of the films compared to the control film (CHT1-S, no silver). A swelling reduction was also observed when the amount of silver in the film was increased (from 0.166 to 8.3 mM). This can be explained by considering that metallic nanoparticles can act as chitosan crosslinkers [40].

Porous chitosan-based scaffolds were also produced by ice template using polymeric solutions with AgNPs at a concentration of 0.83 or 8.3 mM (Fig. S4).

The release of AgNPs in PBS media from the films and the scaffolds at pH 7.4 and 37 °C was studied for 24 h. In all cases, the amount of silver detected by ICP was neglected. Due to the presence of chloride ions in the PBS media, released AgNPs may precipitate in the form of AgCl, so silver ions cannot be detected. Therefore, the experiment was carried out in a phosphate buffer at pH 7.4. At 24 h, the percentage of silver release from films was 10 %, while the release was 14 % for the scaffolds.

3.4. Antimicrobial properties

Chitosan and some chitosan derivatives exhibit antimicrobial activity against many microorganisms, which depends on the polymer's physicochemical properties and the derivatives' chemical nature [17]. The antimicrobial activity of the parent chitosans, chitosan salts and the

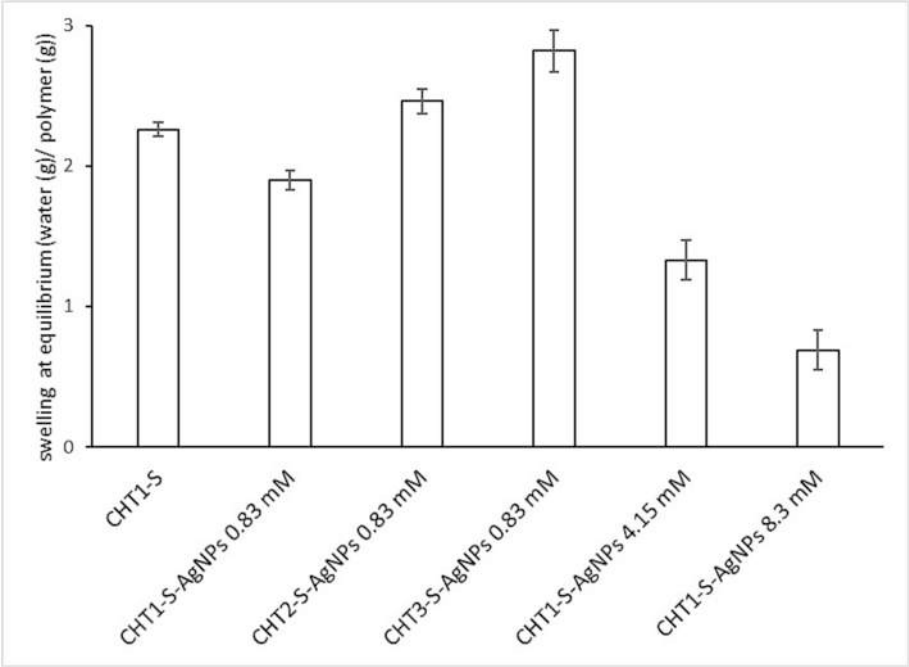

Fig. 5. Film swelling at equilibrium in PBS at 37 °C.

polymeric solutions containing the colloidal AgNPs (0.83 mM) was tested against *Staphylococcus aureus* (Gram-positive) and *Pseudomonas aeruginosa* (Gram-negative) (Table 2). Typically, chitosan has a larger antimicrobial activity against *S. aureus* than *P. aeruginosa,* which is in good agreement with our results. Both chitosan and its salts showed moderate antimicrobial activity against *S. aureus* and *P. aeruginosa,* although in the case of silver concentration MICs and MCBs were lower than those published previously using chitosan-AgNPs [59]. A possible explanation supported by previous studies is that antimicrobial activity is related to the number of sulfopropyl moieties since low chitosan sulfonated samples exhibited higher activity than high sulfonated ones [60].

The antimicrobial activity of the different chitosan films was also tested against *P. aeruginosa* and *S. aureus* in Mueller Hinton agar plates.

Table 2
Antimicrobial activity of chitosan, chitosan derivatives and colloidal AgNPs stabilized with chitosan derivatives solutions against *Staphylococcus aureus* or *Pseudomonas aeruginosa*.

Sample	*S. aureus*		*P. aeruginosa*	
	MIC	MCB	MIC	MCB
CHT1[a]	1	2	2	2
CHT2[a]	1	1	1	4
CHT3[a]	0.5	1	1	4
CHT1-S[a]	2	2	2	>4
CHT2-S[a]	1	2	2	>4
CHT3-S[a]	0.5	1	1	>4
CHT1-S-AgNPs[a]	0.5	0.5	0.5	2
CHT2-S-AgNPs[a]	0.5	1	0.25	1
CHT3-S-AgNPs[a]	0.12	0.5	0.25	2
CHT1-S-AgNPs[b]	2.25	2.25	2.25	9
CHT2-S-AgNPs[b]	2.25	4.5	1.125	4.5
CHT3-S-AgNPs[b]	0.56	2.25	1.125	9

[a] Minimal inhibitory concentration (MIC) and minimal bactericidal concentration (MBC) were calculated on the basis of polymer concentration ($mg{\cdot}mL^{-1}$).
[b] MIC and MBC were calculated on the basis of silver concentration ($\mu g{\cdot}mL^{-1}$).

However, they did not provide conclusive results due to their inability to maintain a regular shape when overlaid on the agar plate (data not shown). Therefore, films harbouring 0.42 or 0.83 μmol AgNPs (silver) were immersed in tubes containing 2 mL of Mueller Hinton broth and inoculated with *S. aureus* or *P. aeruginosa*. Both types of films (0.42 and 0.83 μmol) inhibited the growth of both types of bacteria compared to the control films without AgNPs after 24 h (Fig. 6). Clear tubes showing no growth were analyzed by plating 10-fold dilutions on MH plates. While the number of bacterial cells in either 0.42 or 0.83 μmol $AgNO_3$ solutions was below the level of detection, 0.42 and 0.83 μmol AgNP films only allowed duplication of the initial populations of *P. aeruginosa* or *S. aureus* cells supporting a bacteriostatic effect for AgNP films.

Chitosan versatility allowed us to produce not only films but also scaffolds which increased AgNPs exposition to the media. Scaffolds were prepared from polymer solutions containing a silver concentration of 4.15 and 8.3 mM, respectively. The scaffolds were cut for a final silver content of 0.17 and 0.83 μmol. Both concentrations inhibited bacterial growth when assayed against *P. aeruginosa* or *S. aureus*, while the unloaded scaffolds did not (Fig. 7). To detect a bacteriostatic or bactericidal effect, samples from clear tubes harbouring chitosan, AgNP-scaffolds or Ag^+ solutions were 10-fold diluted and plated onto MH medium. The number of remaining cells in 0.83 μmol samples was below the level of detection, while 0.17 μmol scaffold samples supported a limited growth 5 orders of magnitude lower than the chitosan scaffold counts; a fact that would explain that 24 h later (48 h from the beginning of the experiment) 0.17 μmol scaffold tubes finally showed bacterial growth (Fig. 7). After 120 h of incubation, no further changes were observed (Fig. S5). Therefore, using a 3D scaffold enhanced the effect of the chitosan-AgNPs combination compared to equivalent films previously assayed.

Scaffolds were immersed in MHB to detect a putative release of AgNPs from AgNP-scaffolds that could explain their activities. Samples from the supernatant were taken at different time points and assayed as indicated in the Materials and Methods section. Preliminary results showed that supernatants from 0.83 μmol AgNP-scaffolds inhibited bacterial growth just 30 min after the onset of the experiment (Fig. S6). Released solutions after 24 h had similar inhibitory activity against

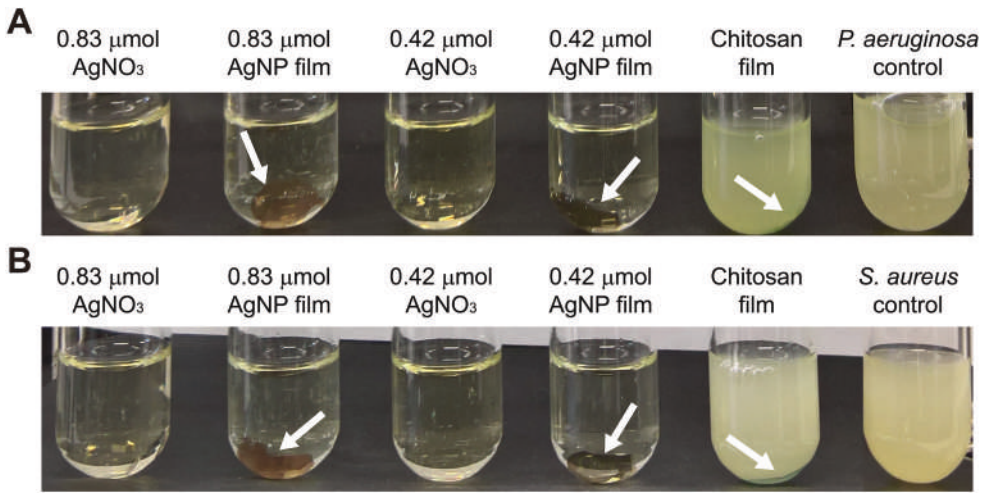

Fig. 6. Bacterial inhibitory activity of chitosan derivatives-based films with AgNPs against *P. aeruginosa* (A) or *S. aureus* (B) in MHB cultures after 24 h of treatment compared to chitosan scaffold or $AgNO_3$ solutions. White arrows indicate films inside the tubes.

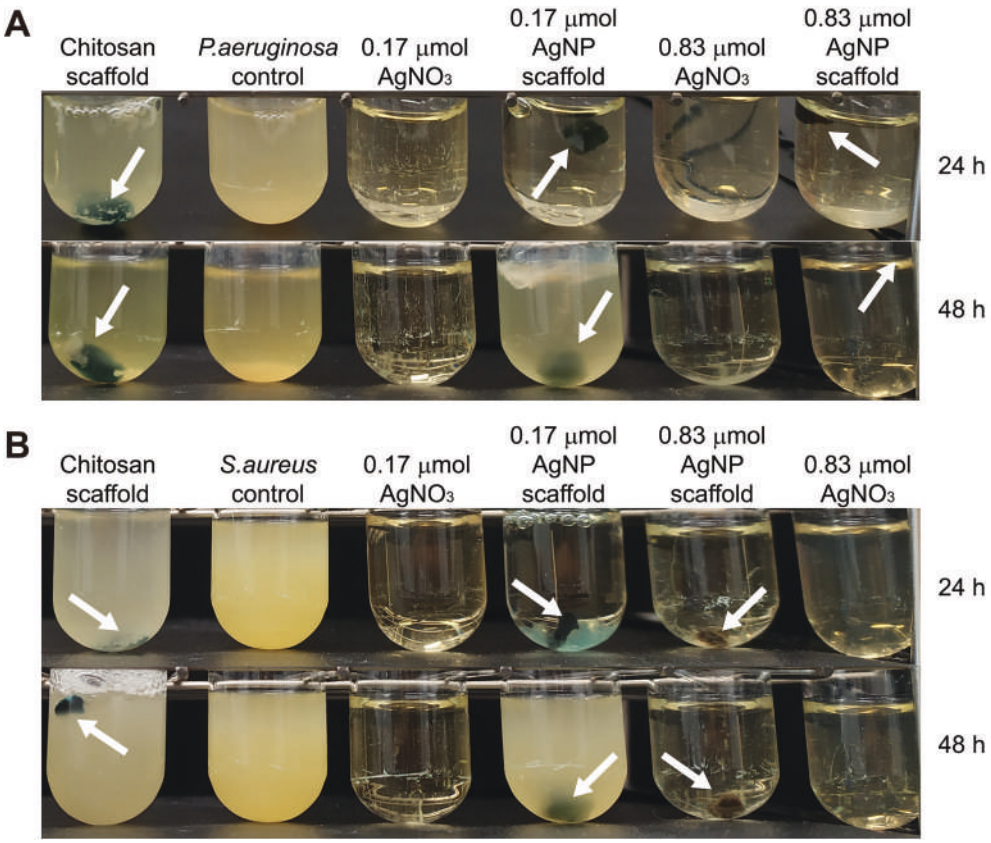

Fig. 7. Bacterial inhibitory activity of chitosan derivatives-based scaffolds with AgNPs against *P. aeruginosa* (A) or *S. aureus* (B) in MHB cultures after 24 h and 48 h of treatment compared to chitosan scaffold or $AgNO_3$ solutions. White arrows indicate scaffolds inside the tubes.

P. aeruginosa and *S. aureus* to that of an equivalent $AgNO_3$ solution (Fig. 8). In addition, solutions recovered from additional periods of release (24 and 48 h) in fresh media showed a progressive increase of inhibitory activity against both bacteria, finally reaching a similar activity to that of the $AgNO_3$ solution.

All these results together support a fast and long-lasting activity of AgNP-chitosan scaffolds that could even be reused several times.

4. Conclusion

In this work, for the first time, the ability of a sulfopropyl chitosan salt demonstrated its ability for the green synthesis of silver nanoparticles. Better control of the morphological properties of the nanoparticles and the use of large silver concentrations than those used with chitosan was observed, particularly when acetic acid is substituted by water. This result highlights the potential use of chitosan derivatives in AgNPs scale-up processes since large silver concentrations in the presence of chitosan tend to form highly viscous solutions or even gels.

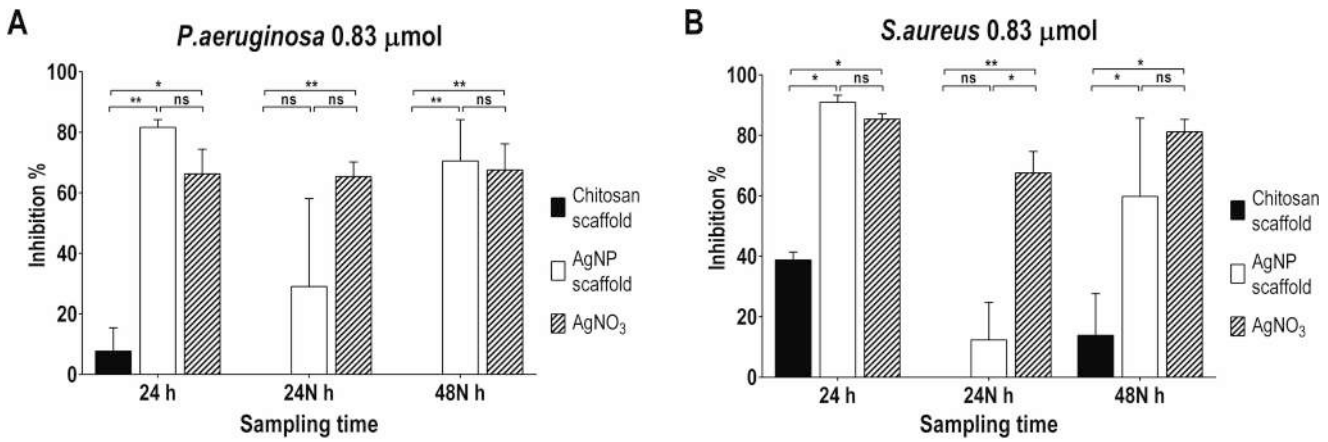

Fig. 8. Inhibitory activity of release solutions of chitosan derivatives-based scaffolds with AgNPs (0.83 µmol, silver) against *P. aeruginosa* (A) or *S. aureus* (B) in MHB broth measured after 10 h of treatment compared to chitosan scaffold or $AgNO_3$ solution (0.83 µmol). *24 h* solution was collected after a 24 h incubation of scaffolds in MHB. After that, scaffolds were rescued, washed and immersed in new MHB for additional periods of 24 h (*24 N h*) and 48 h (*48 N h*). Statistical analysis was achieved using 2-way ANOVA ($n = 3$). Levels of statistically significant differences are indicated as *, $p < 0.05$; **, $p < 0.01$, respectively; or *ns*, not significant. Error bars represent the standard error of the means.

Moreover, for some applications, the control of AgNPs formation is crucial, and water as solvent has proved to be more appropriate to this end. Either films or scaffolds harbouring AgNPs had a bactericidal effect at low concentrations of silver, thus, increasing the therapeutic index compared to precedent formulations of silver nanoparticles.

CRediT authorship contribution statement

I. Aranaz: Conceptualization, Methodology, Investigation, Supervision, Visualization, Writing – original draft, Writing – review & editing. **F. Navarro-García:** Investigation, Methodology, Visualization, Formal analysis, Data curation, Resources, Writing – original draft, Writing – review & editing. **M. Morri:** Investigation. **N. Acosta:** Data curation, Writing – review & editing, Funding acquisition. **L. Casettari:** Writing – review & editing. **A. Heras:** Funding acquisition.

Declaration of competing interest

The authors declare no competing financial interest.

Acknowledgements

Funding

This work was supported by Science, Innovation and Universities Ministry, Spain (grant number PID2019-105337RB-C22) M.M. thanks ERASMUS Programme for Mobility Grant (European Comission).

Appendix A. Supplementary data

Supplementary data to this article can be found online at https://doi.org/10.1016/j.ijbiomac.2023.123849.

References

[1] K. Yamada, The origins of acupuncture, moxibustion, and decoction: the two phases of the formation of ancient medicine, in: International Research Center for Japanese Studies Kyoto, Kyoto, Japan, 1998.
[2] S. Silver, L.T. Phung, Bacterial heavy metal resistance: new surprises, Annu. Rev. Microbiol. 50 (1996) 753–789, https://doi.org/10.1146/annurev.micro.50.1.753.
[3] J.W. Alexander, History of the medical use of silver, Surg. Infect. 10 (2009) 289–292, https://doi.org/10.1089/sur.2008.9941.
[4] W. Sim, R.T. Barnard, M.A.T. Blaskovich, Z.M. Ziora, Antimicrobial silver in medicinal and consumer applications: a patent review of the past decade (2007−2017), Antibiotics 7 (2018), https://doi.org/10.3390/antibiotics7040093.
[5] A. Hamad, K.S. Khashan, A. Hadi, Silver nanoparticles and silver ions as potential antibacterial agents, J. Inorg. Organomet. Polym. Mater. 30 (2020) 4811–4828, https://doi.org/10.1007/s10904-020-01744-x.
[6] S. Iravani, H. Korbekandi, S.V. Mirmohammadi, B. Zolfaghari, Synthesis of silver nanoparticles: chemical, physical and biological methods, Res. Pharm. Sci. 9 (2014) 385–406.
[7] B. Aragaw, M.T. Alula, S. Majoni, C. King'ondu, in: Chemical Synthesis of Silver Nanoparticles, 2022, pp. 21–53, https://doi.org/10.1016/B978-0-12-824508-8.00017-4.
[8] S. Navaladian, B. Viswanathan, R. Viswanath, T. Varadarajan, Thermal decomposition as route for silver nanoparticles, Nanoscale Res. Lett. 2 (2006) 44–48, https://doi.org/10.1007/s11671-006-9028-2.
[9] M. Skiba, V. Vorobyova, Synthesis of silver nanoparticles in a plasma electrochemical system for degradation of environmental pollutants, Mater. Today Proc. 50 (2022) 492–495, https://doi.org/10.1016/j.matpr.2021.11.300.
[10] M. Faried, S. Kamyar, M. Miyake, Z. Zakaria, H. Hara, N. Khairudin, M. Etemadi, Ultrasound-assisted in the synthesis of silver nanoparticles using sodium alginate mediated by green method, Dig. J. Nanomater. Biostruct. 11 (2016) 547–552.
[11] O. Pryshchepa, P. Pomastowski, B. Buszewski, Silver nanoparticles: synthesis, investigation techniques, and properties, Adv. Colloid Interf. Sci. 284 (2020), 102246, https://doi.org/10.1016/j.cis.2020.102246.
[12] H. Huang, X. Yang, Synthesis of polysaccharide-stabilized gold and silver nanoparticles:a green method, Carbohydr. Res. 339 (2004) 2627–2631, https://doi.org/10.1016/j.carres.2004.08.005.
[13] S. Ifuku, Y. Tsukiyama, T. Yukawa, M. Egusa, H. Kaminaka, H. Izawa, M. Morimoto, H. Saimoto, Facile preparation of silver nanoparticles immobilized on chitin nanofiber surfaces to endow antifungal activities, Carbohydr. Polym. 117 (2015) 813–817, https://doi.org/10.1016/j.carbpol.2014.10.042.
[14] P. Raveendran, J. Fu, S.L. Wallen, Completely "green" synthesis and stabilization of metal nanoparticles, J. Am. Chem. Soc. 125 (2003) 13940–13941, https://doi.org/10.1021/ja029267j.
[15] Z. Ma, J. Liu, Y. Liu, X. Zheng, K. Tang, Green synthesis of silver nanoparticles using soluble soybean polysaccharide and their application in antibacterial coatings, Int. J. Biol. Macromol. 166 (2021) 567–577, https://doi.org/10.1016/j.ijbiomac.2020.10.214.
[16] J. Wongpreecha, D. Polpanich, T. Suteewong, C. Kaewsaneha, P. Tangboriboonrat, One-pot, large-scale green synthesis of silver nanoparticles-chitosan with enhanced antibacterial activity and low cytotoxicity, Carbohydr. Polym. 199 (2018) 641–648, https://doi.org/10.1016/j.carbpol.2018.07.039.
[17] I. Aranaz, M. Mengíbar, R. Harris, B. Miralles, N. Acosta, L. Calderón, Á. Sánchez, Á. Heras, Role of physicochemical properties of chitin and chitosan on their functionality, Curr. Chem. Biol. 8 (2014).
[18] N. Bhattarai, J. Gunn, M. Zhang, Chitosan-based hydrogels for controlled, localized drug delivery, Adv. Drug Deliv. Rev. 62 (2010) 83–99, https://doi.org/10.1016/j.addr.2009.07.019.
[19] F. Croisier, C. Jérôme, Chitosan-based biomaterials for tissue engineering, Eur. Polym. J. 49 (2013) 780–792, https://doi.org/10.1016/j.eurpolymj.2012.12.009.
[20] M.Z. Elsabee, E.S. Abdou, Chitosan based edible films and coatings: a review, Mater. Sci. Eng. C 33 (2013) 1819–1841, https://doi.org/10.1016/j.msec.2013.01.010.
[21] C.K.S. Pillai, W. Paul, C.P. Sharma, Chitin and chitosan polymers: chemistry, solubility and fiber formation, Prog. Polym. Sci. 34 (2009) 641–678, https://doi.org/10.1016/j.progpolymsci.2009.04.001.
[22] A. Rampino, M. Borgogna, P. Blasi, B. Bellich, A. Cesàro, Chitosan nanoparticles: preparation, size evolution and stability, Int. J. Pharm. 455 (2013) 219–228, https://doi.org/10.1016/j.ijpharm.2013.07.034.

[23] M. Tiboni, E. Elmowafy, M.O. El-Derany, S. Benedetti, R. Campana, M. Verboni, L. Potenza, F. Palma, B. Citterio, M. Sisti, A. Duranti, S. Lucarini, M.E. Soliman, L. Casettari, A combination of sugar esters and chitosan to promote in vivo wound care, Int. J. Pharm. 616 (2022), 121508, https://doi.org/10.1016/j.ijpharm.2022.121508.
[24] The United States Pharmacopeia 34/National Formulary 29, 2011.
[25] Council of Europe, in: European Pharmacopeia 9.8, 2019, pp. 2028–2029.
[26] V.K. Mourya, N.N. Inamdar, Trimethyl chitosan and its applications in drug delivery, J. Mater. Sci. Mater. Med. 20 (2008) 1057, https://doi.org/10.1007/s10856-008-3659-z.
[27] W. Wang, Q. Meng, Q. Li, J. Liu, M. Zhou, Z. Jin, K. Zhao, Chitosan derivatives and their application in biomedicine, Int. J. Mol. Sci. 21 (2020), https://doi.org/10.3390/ijms21020487.
[28] C.L. Chen, Y.M. Wang, C.F. Liu, J.Y. Wang, The effect of water-soluble chitosan on macrophage activation and the attenuation of mite allergen-induced airway inflammation, Biomaterials 29 (2008) 2173–2182, https://doi.org/10.1016/j.biomaterials.2008.01.023.
[29] M.A. Huq, M. Ashrafudoulla, M.A.K. Parvez, S.R. Balusamy, M.M. Rahman, J. H. Kim, S. Akter, Chitosan-coated polymeric silver and gold nanoparticles: biosynthesis,characterization and potential antibacterial applications: a review, Polymers (Basel) 14 (2022), https://doi.org/10.3390/polym14235302.
[30] P. Senthilkumar, G. Yaswant, S. Kavitha, E. Chandramohan, G. Kowsalya, R. Vijay, B. Sudhagar, D.S.R.S. Kumar, Preparation and characterization of hybrid chitosan-silver nanoparticles (Chi-Ag NPs); a potential antibacterial agent, Int. J. Biol. Macromol. 141 (2019) 290–298, https://doi.org/10.1016/j.ijbiomac.2019.08.234.
[31] O.A. Douglas-Gallardo, C.A. Christensen, M.C. Strumia, M.A. Pérez, C.G. Gomez, Physico-chemistry of a successful micro-reactor: random coils of chitosan backbones used to synthesize size-controlled silver nanoparticles, Carbohydr. Polym. 225 (2019), 115241, https://doi.org/10.1016/j.carbpol.2019.115241.
[32] D. Wei, W. Sun, W. Qian, Y. Ye, X. Ma, The synthesis of chitosan-based silver nanoparticles and their antibacterial activity, Carbohydr. Res. 344 (2009) 2375–2382, https://doi.org/10.1016/j.carres.2009.09.001.
[33] I. Aranaz, C. Castro, A. Heras, N. Acosta, On the ability of low molecular weight chitosan enzymatically depolymerized to produce and stabilize silver nanoparticles, Biomimetics 3 (2018), https://doi.org/10.3390/biomimetics3030021.
[34] V. Kulikouskaya, K. Hileuskaya, A. Kraskouski, I. Kozerozhets, E. Stepanova, I. Kuzminski, L. You, V. Agabekov, Chitosan-capped silver nanoparticles: a comprehensive study of polymer molecular weight effect on the reaction kinetic, physicochemical properties, and synergetic antibacterial potential, SPE Polym. 3 (2022) 77–90, https://doi.org/10.1002/pls2.10069.
[35] O. Velgosová, A. Mražíková, R. Marcinčáková, Influence of pH on green synthesis of Ag nanoparticles, Mater. Lett. 180 (2016) 336–339, https://doi.org/10.1016/j.matlet.2016.04.045.
[36] M.K. Alqadi, O.A.Abo Noqtah, F.Y. Alzoubi, J. Alzouby, K. Aljarrah, pH effect on the aggregation of silver nanoparticles synthesized by chemical reduction, Mater. Sci. 32 (2014) 107–111, https://doi.org/10.2478/s13536-013-0166-9.
[37] Y.-K. Twu, Y.-W. Chen, C.-M. Shih, Preparation of silver nanoparticles using chitosan suspensions, Powder Technol. 185 (2008) 251–257, https://doi.org/10.1016/j.powtec.2007.10.025.
[38] R. Kalaivani, M. Maruthupandy, T. Muneeswaran, A. Hameedha Beevi, M. Anand, C.M. Ramakritinan, A.K. Kumaraguru, Synthesis of chitosan mediated silver nanoparticles (Ag NPs) for potential antimicrobial applications, Front. Lab. Med. 2 (2018) 30–35, https://doi.org/10.1016/j.flm.2018.04.002.
[39] A. Lunkov, B. Shagdarova, M. Konovalova, Y. Zhuikova, N. Drozd, A. Il'ina, V. Varlamov, Synthesis of silver nanoparticles using gallic acid-conjugated chitosan derivatives, Carbohydr. Polym. 234 (2020), 115916, https://doi.org/10.1016/j.carbpol.2020.115916.
[40] D. Silvestri, S. Wacławek, A. Venkateshaiah, K. Krawczyk, B. Sobel, V.V.T. Padil, M. Černík, R.S. Varma, Synthesis of ag nanoparticles by a chitosan-poly(3-hydroxybutyrate) polymer conjugate and their superb catalytic activity, Carbohydr. Polym. 232 (2020), 115806, https://doi.org/10.1016/j.carbpol.2019.115806.
[41] Y. Liu, Z. Sun, L. Xiu, J. Huang, F. Zhou, Selective antifungal activity of chitosan and sulfonated chitosan against postharvest fungus isolated from blueberry, J. Food Biochem. 42 (2018), e12658, https://doi.org/10.1111/jfbc.12658.
[42] Y. Liu, Y. Jiang, J. Zhu, J. Huang, H. Zhang, Inhibition of bacterial adhesion and biofilm formation of sulfonated chitosan against Pseudomonas aeruginosa, Carbohydr. Polym. 206 (2019) 412–419, https://doi.org/10.1016/j.carbpol.2018.11.015.
[43] A. Heydari, M. Darroudi, I. Lacík, Efficient N-sulfopropylation of chitosan with 1,3-propane sultone in aqueous solutions: neutral pH as the key condition, React. Chem. Eng. 6 (2021) 2146–2158, https://doi.org/10.1039/d1re00089f.
[44] G.G. Allan, M. Peyron, Molecular weight manipulation of chitosan I: kinetics of depolymerization by nitrous acid, Carbohydr. Res. 277 (1995) 257–272, https://doi.org/10.1016/0008-6215(95)00207-A.
[45] H.S. Hirano, Y. Ohe, Ono, selective N-acylation of chitosan, Carbohydr. Res. 47 (1976) 315–320. https://www.sciencedirect.com/science/article/abs/pii/S0008621500841981.
[46] R.A. Muzzarelli, R. Rochetti, V. Stanic, M. Weckx, R. Roccheti, V. Stanic, M. Weckx, Methods for the determination of the degree of acetylation of chitin and chitosan, in: R.A. Muzarelli, M.G. Peter (Eds.), Chitin Handb, Atec Edizioni, Grottammare, Italy, 1997, pp. 109–119.
[47] M. Rinaudo, M. Milas, P. Le Dung, Characterization of chitosan. Influence of ionic strength and degree of acetylation on chain expansion, Int. J. Biol. Macromol. 15 (1993) 281–285.
[48] A. Blanco, A. García-Abuín, D. Gómez-Díaz, J.M. Navaza, Physicochemical characterization of chitosan derivatives, CyTA - J. Food 11 (2013) 190–197, https://doi.org/10.1080/19476337.2012.722565.
[49] S.E. Lasker, S.S. Stivala, Physicochemical studies of fractionated bovine heparin: I. Some dilute solution properties, Arch. Biochem. Biophys. 115 (1966) 360–372.
[50] M.H. Struszczyk, Microcrystalline chitosan. I. Preparation and properties of microcrystalline chitosan, J. Appl. Polym. Sci. 33 (1987) 177–189.
[51] CLSI, Performance Standards for Antimicrobial Susceptibility Testing; Twenty-Fourth Informational Supplement. CLSI document M100-S24 (ISBN 1-56238-897-5 [Print]; ISBN 1-56238-898-3 [Electronic]), 2014.
[52] G.A.F. Roberts, Derivatives of chitin and chitosan, in: Chitin Chem, Macmillan, 1992, p. 184.
[53] Z. Sun, C. Shi, X. Wang, Q. Fang, J. Huang, Synthesis, characterization, and antimicrobial activities of sulfonated chitosan, Carbohydr. Polym. 155 (2017) 321–328, https://doi.org/10.1016/j.carbpol.2016.08.069.
[54] J. Kumirska, M. Czerwicka, Z. Kaczyński, A. Bychowska, K. Brzozowski, J. Thöming, P. Stepnowski, Application of spectroscopic methods for structural analysis of chitin and chitosan, Mar. Drugs 8 (2010) 1567–1636, https://doi.org/10.3390/md8051567.
[55] J. Yang, K. Luo, D. Li, S. Yu, J. Cai, L. Chen, Y. Du, Preparation, characterization and in vitro anticoagulant activity of highly sulfated chitosan, Int. J. Biol. Macromol. 52 (2013) 25–31, https://doi.org/10.1016/j.ijbiomac.2012.09.027.
[56] R. Xing, S. Liu, H. Yu, Z. Guo, Z. Li, P. Li, Preparation of high-molecular weight and high-sulfate content chitosans and their potential antioxidant activity in vitro, Carbohydr. Polym. 61 (2005) 148–154, https://doi.org/10.1016/j.carbpol.2005.04.007.
[57] C.G.T. Neto, J.A. Giacometti, A.E. Job, F.C. Ferreira, J.L.C. Fonseca, M.R. Pereira, Thermal analysis of chitosan based networks, Carbohydr. Polym. 62 (2005) 97–103, https://doi.org/10.1016/j.carbpol.2005.02.022.
[58] J. Annamalai, T. Nallamuthu, Green synthesis of silver nanoparticles: characterization and determination of antibacterial potency, Appl. Nanosci. 6 (2016) 259–265, https://doi.org/10.1007/s13204-015-0426-6.
[59] E.D. Cavassin, L.F.P. de Figueiredo, J.P. Otoch, M.M. Seckler, R.A. de Oliveira, F. F. Franco, V.S. Marangoni, V. Zucolotto, A.S.S. Levin, S.F. Costa, Comparison of methods to detect the in vitro activity of silver nanoparticles (AgNP) against multidrug resistant bacteria, J. Nanobiotechnol. 13 (2015) 64, https://doi.org/10.1186/s12951-015-0120-6.
[60] C.-S. Chen, W.-Y. Liau, G.-J. Tsai, Antibacterial effects of N-sulfonated and N-sulfobenzoyl chitosan and application to oyster preservation, J. Food Prot. 61 (1998) 1124–1128, https://doi.org/10.4315/0362-028X-61.9.1124.